The Fermilab Short-Baseline Program: MicroBooNE

Anne Schukraft[1] for the MicroBooNE Collaboration

[1]*Fermi National Accelerator Laboratory,*
PO Box 500, Batavia IL 60510, U.S.A.

E-mail: aschu@fnal.gov

(Received February 2, 2016)

The MicroBooNE experiment is the first of three detectors of the Fermilab short-baseline neutrino program that started operation in the Booster Neutrino Beamline in October 2015 [1]. When completed, the three-detector lineup will explore short-baseline neutrino oscillations and will be sensitive to sterile neutrino scenarios. MicroBooNE in itself is now starting its own physics program, with the measurement of neutrino-argon cross sections in the $\sim$ 1 GeV range being one of its main physics goals. These proceedings describe the status of the detector, the start of operation, and the automated reconstruction of the first neutrino events observed with MicroBooNE. Prospects for upcoming cross section measurements are also given.

KEYWORDS: Liquid argon time projection chamber, Neutrino-nucleon cross sections

1. The MicroBooNE experiment

The MicroBooNE detector is located in the Booster Neutrino Beamline (BNB) at Fermilab at a baseline of 470 m and contains an active mass of 89 tons. Together with a near detector (SBND) at 112 m (112 tons active mass) and a far detector (ICARUS) at 660 m baseline (476 tons active mass), the neutrino oscillation spectrum will be probed at multiple distances in order to search for a contribution from sterile neutrinos [1]. While the MicroBooNE detector has been taking data since 2015, the SBND and the ICARUS detector will be deployed in the beamline at a later stage.

1.1 Physics goals

One of the two major goals of the detector is the investigation of the low-energy electromagnetic event excess reported by the MiniBooNE experiment [2]. A yet unanswered question is if the observed electromagnetic event excess was caused by electrons or photons, which in MiniBooNE – a mineral oil-filled Cherenkov detector – were very difficult to distinguish; on the contrary, MicroBooNE will provide very good separation power between electrons and photons, as demonstrated by the ArgoNeuT detector [3].

The second major physics goal of MicroBooNE is to measure neutrino-argon cross sections. This is a topical subject and in particular relevant since liquid argon is the target of choice for many future experiments such as the Deep Underground Neutrino Experiment (DUNE) [5]. Located in the Booster Neutrino Beamline [6], which is delivering muon neutrinos with an average energy of 800 MeV, MicroBooNE will accumulate a large statistical data set of quasi-elastic and resonant interactions. Since MicroBooNE is in the same neutrino beamline as the MiniBooNE detector, it will be able to further explore the nuclear effects [4] exposed by MiniBooNE [7], with the difference of a variation of target, which in MicroBooNE is argon instead of carbon. This is expected to contribute to the advancement of theoretical models and neutrino event generators.

Other physics goals of MicroBooNE – not futher discussed in these proceedings – are the characterization of LArTPC detector properties, the detection of supernova neutrinos and the exploration

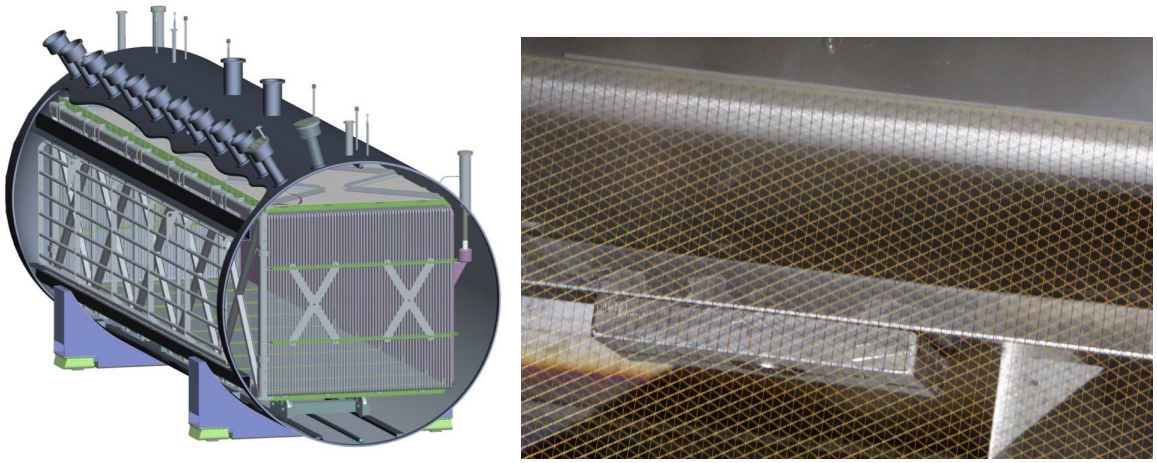

Fig. 1. Left: schematic drawing of the MicroBooNE cryostat holding the TPC. The anode wires planes are on the left hand side of the cryostat. The nozzles carry electronic readout cables, and provide access for the cathode high-voltage, the calibration lasers, purity monitors, and cryogenic services. Right: A photograph of the anode wire planes showing the three layers of wires crossing in a 60° angle [9]. The spacing of the wires is 3 mm.

of regimes of new physics such as nucleon decay, and dark sector models. Many of these studies are being performed in preparation for DUNE.

1.2 Detector

The MicroBooNE liquid argon time projection chamber (LArTPC) has an active volume of about 89 tons with dimensions of 10 m in beam direction, 2.3 m height, and 2.5 m drift distance between the cathode plane and the anode wire planes [8]. Charged particles produced in neutrino interactions inside the liquid argon ionize the argon atoms; the ionization electrons drift towards the anode planes where they leave a projected image of the particle trajectories that is read out. The anode consists of three different planes of wires. The ionization electrons leave an induction signal when passing through the first two planes of wires and are then collected on the third wire plane. The spacing between the wires as well as between the wire planes is 3 mm, which defines the resolution of the projected image. The wire planes are rotated 60° with respect to one another (see Fig. 1). The wires are gold-coated stainless steel, and in total the detector is instrumented with over 8000 of these.

The TPC is housed in a cryostat that holds a total mass of 170 tons of liquid argon. The argon is kept at a temperature of 87 K and is constantly purified. The cryostat was welded shut, allowing very limited physical access [9]. Multiple service nozzles on the cryostat allow the exchange of electrical signals between the different detector components and the outside of the cryostat.

In addition to the TPC system, that is recording the ionization signal produced by the neutrino interaction and secondary particles, the detector is equipped with a light system, that is collecting the emitted scintillation light. The light system consists of 32 8-inch photomultiplier tubes (PMTs) that are mounted on the cryostat wall behind the anode wire planes. In front of the PMTs are wavelength shifting plates that shift the argon scintillation light from a wavelength of 128 nm to a wavelength in the operational region of the PMTs [10]. The prompt light measured by the PMTs provides a start time for the drift electrons that allows the reconstruction of the third space coordinate based on the arrival time of the drift electrons at the wire planes. This is important, since the drift electrons are very slow relative to the prompt light signal, and therefore only the light can be used for triggering on beam neutrino events, as will be explained in Section 2.

An important element of the MicroBooNE program is that it also serves as important R&D for fu-

ture short and long-baseline neutrino detectors. Several of the detector components and technologies in MicroBooNE are new developments, such as the cold electronics for the wire readout, which is operating completely submerged in the liquid argon [11]. With 2.5 m, MicroBooNE also has a longer drift length than previous liquid argon neutrino detectors, addressing the challenge of applying high electric potential to obtain the required electric drift field [12]. In order to protect components in the case of electric breakdown, surge protection devices were implemented in MicroBooNE, the first for a LArTPC [14, 15]. A new technology in use is also the laser system for the calibration of the electric field in MicroBooNE [16]. All detector systems were fully commissioned and operational in summer 2015.

2. Automated reconstruction and selection of the first neutrino events in MicroBooNE

Since October 15, 2015, MicroBooNE has been receiving beam spills from the BNB with a rate of up to 5 Hz and 4.6×10^{12} protons on target (POT) per spill. Since the MicroBooNE detector is near the surface, the rate of cosmic ray induced backgrounds is much higher than the rate of interacting neutrinos. Therefore, a fully automated reconstruction and selection of events is required. The following sections describe how MicroBooNE's first neutrino candidate events were identified with a fully automated procedure.

Assuming a normal BNB intensity of 4×10^{12} POT per beam spill, the chances that a neutrino interaction occurs inside the detector active volume is about one in 660 beam spills. At the start of operation, the arrival of any beam spill of a length of 1.6 μs communicated through a signal from the accelerator complex triggers the readout of an event. The event duration is 4.8 ms in order to comfortably allow drift electrons to cross the entire drift distance. The maximum drift time for a distance of 2.5 m at a cathode high voltage of 70 kV is about 2.3 ms. Within this readout window, there are typically several tens of cosmic muon tracks on top of the neutrino interaction, if one is present.

The selection of neutrino candidates among these events happens in two steps: First, the light system is used in order to select only events with a scintillation light signal that can be correlated with the beam spill time. The second step is to fully reconstruct these events in 3D and select neutrino candidate events based on their topology. These steps are further outlined in the following subsections.

2.1 Time-based selection of neutrino events

The duration of a beam spill is 1.6 μs. This is very short compared to the entire readout time window of 4.8 ms. Since a component of the scintillation light from the neutrino interaction is prompt, events that do not have a light signal within these 1.6 μs are immediately rejected.

The optical reconstruction starts with selecting pulses on the individual PMTs. Pulses correlated in time across the PMTs are grouped into so called optical flashes, which are characterized by a total charge, start time, and width. For this selection of the first neutrino events in MicroBooNE, the threshold is set to flashes with more than 50 photoelectrons, in order to suppress noise and other backgrounds. At the very start of detector operation, the start of the beam spill window with respect to the trigger signal received from the accelerator complex had to be determined in order to apply an appropriate timing cut. This time offset can only be calibrated using neutrino interactions by looking at the distribution of flashes above threshold as a function of time, which is shown in Fig. 2. An irreducible constant background rate is caused by cosmic muons in accidental coincidence with the beam spill window. The excess above background level, seen between 3 μs and 5 μs, shows the neutrinos from the BNB. Rejecting events without an optical signal during this time window allows less than 1% of background events to pass. This rate is measured from off-beam data. Monte Carlo studies indicate that more than 80% of neutrino interactions pass the charge threshold of 50 photoelectrons and the

timing cut. Fig. 2 is also the first evidence of neutrino interactions in the MicroBooNE detector.

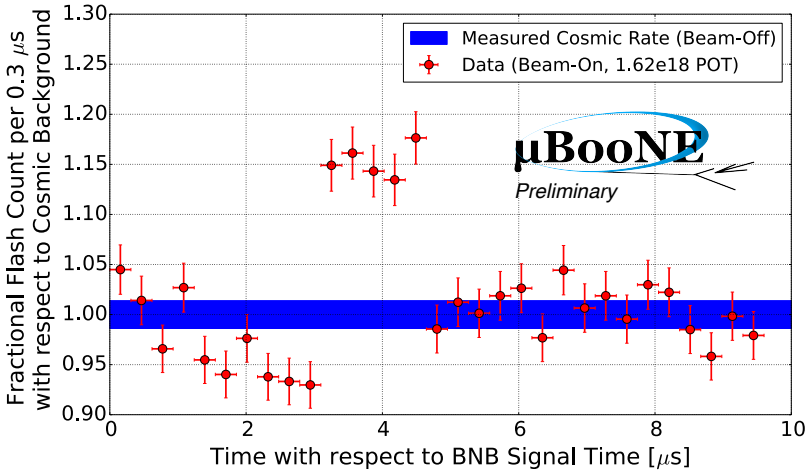

Fig. 2. The ratio to a flat cosmogenic background (measured in a high-statistics beam-off sample), of the number of flashes per 0.3 μs as a function of time with respect to trigger time. Data from the first week, totaling 1.62×10^{18} protons on target (POT) were collected and PMT flashes below 50 photoelectrons were discarded. The remainder of PMT flashes were included in this plot. There is a clear excess due to beam events seen between 3 μs and 5 μs after the beam trigger, which is caused by BNB neutrino interactions.

The optical selection results in a neutrino-enhanced sample. Fig. 2 shows that the neutrino contribution is around 15% and the sample is still background dominated at this stage.

2.2 Topological selection of neutrino events

In order to further reduce cosmic backgrounds and select neutrino interactions, events passing the optical cuts are reconstructed in three dimensions. For the purpose of finding the first neutrino interactions in MicroBooNE, the events are searched for two or more tracks, which have their start points within less than 5 cm from each other and originate from a common reconstructed vertex. Additionally, these two tracks must be fully contained in the detector volume (their start- and end-points must be more than 10 cm from all TPC boundaries). Therefore, they must not be vetoed by our cosmic-ray tagging algorithms which identify tracks that pass through detector boundaries or that are clearly out-of-time with the trigger. The longest of the two tracks in the reconstructed interaction must have a small angle ($\cos\theta < 0.85$) with respect to the beam axis, further reducing the likelihood that an incoming cosmic-ray muon is selected.

The reconstruction chain [17] in MicroBooNE starts with the analysis of the electronic signals from each of the sense-wires. After running a noise filter, so called hits are extracted on each wire. Hits are the reconstructed objects of the pulses seen on the wires. These pulses are bi-polar in the case of the first two wire planes, which are induction planes, and unipolar for the last plane reached by the drift electrons, where the electrons are collected on the wires. Hits are characterized by a start time and deposited charge. Further, the hits are grouped into clusters within each plane, based on their position in space (wire number) and time. These clusters already represent two-dimensional projections of particle trajectories within the representation of time – which corresponds to the drift distance – and wire number. In order to obtain three-dimensional images, the two-dimensional information is matched between the planes. Clusters in different planes that can be correlated in time and space, are reconstructed as three-dimensional objects such as tracks and showers.

MicroBooNE Preliminary
1.86×10^{18} POT, BNB

First ν identification

Number of events	Automated event selection Optical + 3D-based
Non-beam background (expected)	4.6 ± 2.6
Total observed	18

Table I. Total number of events that pass the optical cuts and the 3D topological selection, along with the expected background of non-beam-induced interaction events. The results use an integrated 1.86×10^{18} protons on target from the BNB. Uncertainties on the background are statistical only.

The reconstruction and selection was run on the first data collected with the BNB, corresponding to 1.86×10^{18} POT. The same reconstruction and selection was also applied to data taken while the beam was off in order to get a data-driven estimate of background. The event counts are listed in Tab. 2.2. Comparing the on-beam and off-beam event counts of 18 versus 4.6 ± 2.6, there is an excess of selected neutrino candidate events in the on-beam sample. Example event displays of some of these events are shown in Fig. 3. The event displays show the two-dimensional view of wire number on the horizontal axis and time on the vertical axis. Such two-dimensional views exist for all three planes for each event. An alternative neutrino selection algorithm based on the two-dimensional event information has also been developed and applied. However, as expected, the two-dimensional selection results in a sample with a lower neutrino purity. For future neutrino physics analyses, different selections with a higher selection efficiency are being developed.

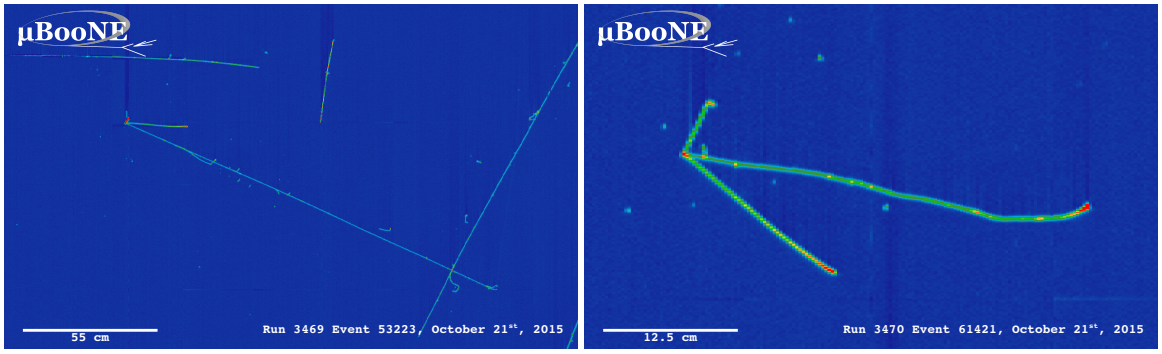

Fig. 3. Example event displays of the first automatically selected neutrino interaction candidate events in MicroBooNE. Both images are collection plane views and show wire number (corresponding to distance in beam direction) on the horizontal axis and time (corresponding to distance in drift direction) on the vertical axis. The beam is entering from the left. The color indicates the deposited charge.

3. Outlook on MicroBooNE cross section measurements

3.1 Predicted event rates in MicroBooNE

MicroBooNE is taking data with liquid argon as a target, the same neutrino target as in the ArgoNeuT experiment but at a lower neutrino energy. The neutrino energy spectrum is the same

MicroBooNE Simulation preliminary
1×10^{20} POT, BNB

Final state	Events
CC inclusive	26500
CC 0π	17000
NC elastic	2600
NC single π^0	1700
NC single γ	20

Table II. Neutrino interactions expected in the MicroBooNE detector for 1×10^{20} POT and 87 tons mass. Selection efficiencies and acceptance are not considered.

as in MiniBooNE, which will allow comparisons between argon and carbon as a target. Fig. 4 shows a distribution of neutrino events expected in the MicroBooNE active volume simulated with GENIE [18]. The neutrino energies peak around 1 GeV, and the majority of collected events will be produced in charged-current (CC) quasi-elastic processes, followed by resonant production. The number of expected events per experimentally observable final state as a function of the accumulated protons on target (POT) is also given in Fig. 4. By the end of 2015, MicroBooNE had received just above 1×10^{20} POT from the BNB. Based on MC estimates, this corresponds to the event numbers shown in Tab. II.

For the ν_μ CC inclusive channel, this data set already corresponds to more than six times the number of events ArgoNeuT had available for their pioneering measurements of CC inclusive neutrino cross sections on argon [19, 21]. See Section 3.2 for MicroBooNE's studies towards a first CC inclusive measurement. For a signal sample including a single muon and any number of nucleons in the final state (CC 0π), MicroBooNE has already accumulated more than 20 times the statistics that ArgoNeuT used for the first analysis of this channel on argon presented at this conference [22]. This is due to the lower energy of the BNB, which enhances statistics for quasi-elastic processes. This channel is of great interest to study nuclear effects and compare to measurements performed by other experiments such as MiniBooNE [20]. With the large statistical sample collected by MicroBooNE, the first precision measurements on an argon target can be performed.

The channel of neutral current (NC) single π^0 events is of great importance since the signature constitutes a background for the search for single electron showers from ν_e interactions, which could be an oscillation signal. Therefore, a precise measurement of the NC single π^0 cross section on argon is desired. ArgoNeuT's first measurement of this cross section is largely statistics limited with only 123 events in the final sample [23], and MicroBooNE will quickly be able to produce a more precise measurement. At the time of the proceedings, this data has not yet been fully analyzed, but various analyses are in preparation.

3.2 Preview on a first ν_μ charged-current inclusive measurement

MicroBooNE's first cross section measurement is likely to be the measurement of the CC inclusive cross section of ν_μ on argon. There are several reasons for this: (1) this is the channel with highest statistics, (2) it only requires the identification of single muon tracks, which is a relatively simple topology for this type of detector, and (3) this selection serves as a pre-selection for all other subsequent ν_μ CC cross section channels.

As mentioned above, the challenge in MicroBooNE being a surface detector is the removal of cosmic muon tracks. The selection involves applying the optical and 3D track based cosmic tagging tools already explained above, and further selecting single tracks starting within 5 cm of a reconstructed vertex candidate with a minimum track length of 75 cm as muon candidates from a CC

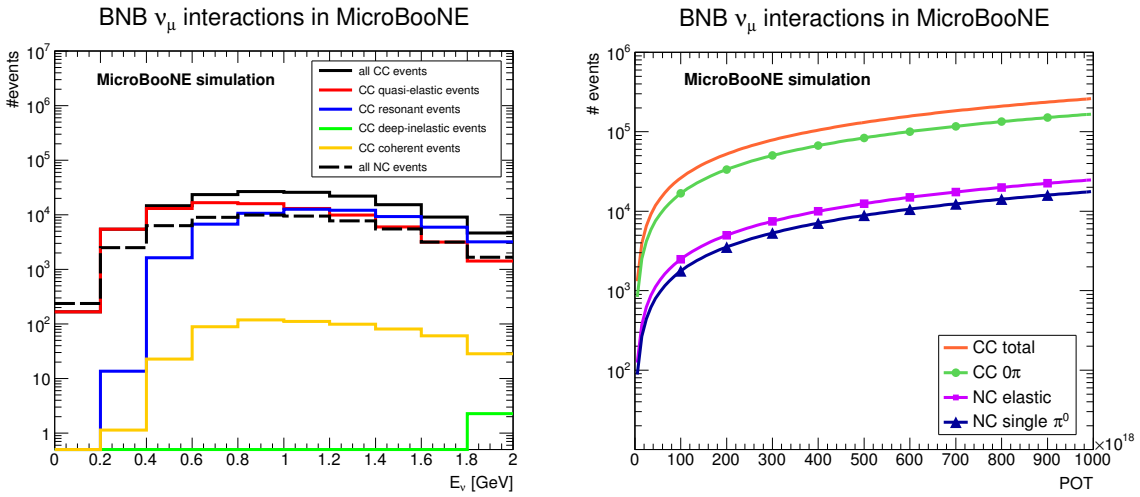

Fig. 4. Left: Energy distribution of BNB muon neutrino event rates in MicroBooNE for different interaction channels for 6.6×10^{20} POT. Right: Cumulative event rates of BNB muon neutrinos in MicroBooNE for different event signatures as a function of protons on target. In both plots, the active volume is 87 tons and selection efficiencies are not considered.

neutrino interaction. With an initial 5.3×10^{19} POT, which is about half the data MicroBooNE had accumulated by the end of 2015, a sample of 4100 ν_μ CC events is selected. The efficiency and acceptance add to being about 30%, which is due to the stringent cosmic tagging cuts requiring full containment of the muon. The remaining number of cosmic muon background tracks is of the same order as the signal. This background is going to be measured and will be subtracted.

The dominant systematic uncertainty for this measurement is the uncertainty on the BNB flux normalization, which is expected to be of the order of 12%. Based on this MC study, a cross section prediction has been extracted and is shown in Fig. 5. The total uncertainty gives an indication of the precision that MicroBooNE will be able to provide. Already with the small amount of statistics used here, the resulting flux-integrated cross section will be systematics dominated. Beyond this, MicroBooNE will be able to quickly perform single differential cross section measurements, e.g., as a function of muon kinematics.

Work on improving the reconstruction and selection, in particular in order to refine the cosmic tagging and increase the neutrino selection efficiency, is ongoing.

4. Summary

As of fall 2015 MicroBooNE is fully operational and taking neutrino data. As has been shown at this conference, the first neutrino interactions have been reconstructed and selected out of the background of cosmic muon tracks. This is the first time automatic reconstruction and neutrino event selection has been demonstrated with a LArTPC located at the surface. An extensive cross section program is now under way. MicroBooNE will soon provide the most precise measurements for neutrino interactions on an argon target.

References

[1] R. Acciarri et al., arXiv:1503.01520 (2015).
[2] The MiniBooNE Collaboration, Phys. Rev. Lett. **102** 101802 (2009).

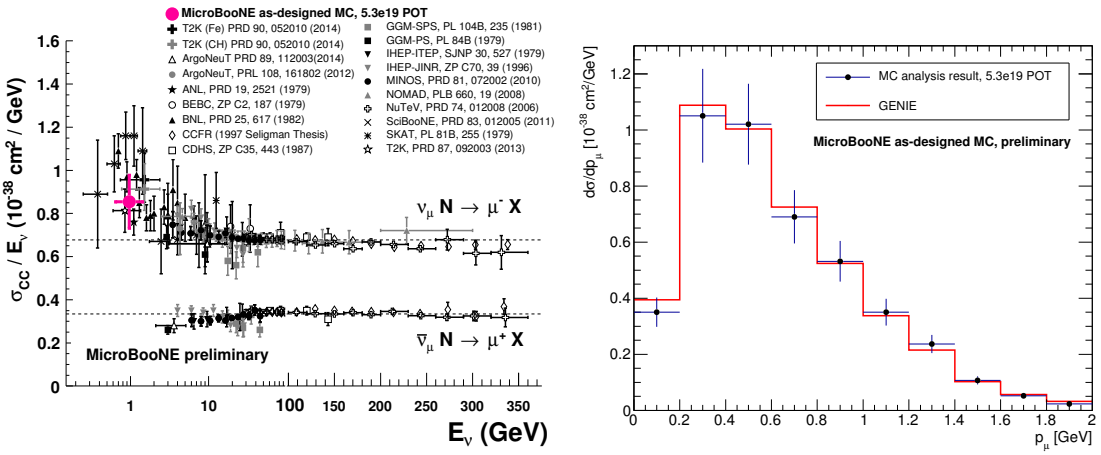

Fig. 5. Left: MicroBooNE flux-integrated ν_μ CC cross section prediction derived from an as-designed detector MC compared to other data [24]. Right: Differential cross section as a function of muon momentum. The MC points with uncertainties are the results extracted after event selection, background subtraction, unsmearing and efficiency correction, assuming an as-designed detector. The uncertainties contain statistical and systematic uncertainties. The red histogram is the prediction obtained directly from the original GENIE simulation, plotted as a function of true muon momentum.

[3] A. M. Szelc, AIP Conf. Proc. **1666** 180001 (2015).
[4] L. Alvarez-Ruso, Y. Hayato, J. Nieves, New J. Phys. **16** 075015 (2014).
[5] The DUNE Collaboration, arXiv:1512.06148 (2015).
[6] The MiniBooNE Collaboration, Phys. Rev. D**79** 072002 (2009).
[7] The MiniBooNE Collaboration, Phys. Rev. D**81** 092005 (2010).
[8] The MicroBooNE Collaboration, *Technical Design Report*, `http://www-microboone.fnal.gov/publications/TDRCD3.pdf`.
[9] B. Carls et al., JINST **10** T08006 (2015).
[10] B. J. P. Jones et al., JINST **8** P01013 (2013).
[11] H. Chen et al., Physics Procedia **37** 1287-1294 (2012).
[12] R. Acciarri et al., JINST **9** P11001 (2014).
[13] M. Auger et al., JINST **9** P07023 (2014).
[14] L. F. Bagby et al., JINST **9** T11004 (2014).
[15] J. Asaadi et al., JINST **9** P09002 (2014).
[16] A. Ereditato et al., JINST **9** T11007 (2014).
[17] E. D. Church, arXiv:1311.6774 [physics.ins-det].
[18] C. Andreopoulos et al., NIM A **614** 87-104 (2010).
[19] R. Acciarri et al., Phys. Rev. Lett. **108** 161802 (2012).
[20] A. A. Aguilar-Arevalo, Pys. Rev. D **81** 092005 (2010).
[21] R. Acciarri et al., Phys. Rev. D **89** 112003 (2014).
[22] O. Palamara, these proceedings (2016).
[23] R. Acciarri et al., arXiv:1511.00941 (2015).
[24] K. A. Olive et al. (Particle Data Group), Chin. Phys. C **38** 090001 (2014).